

A Novel Seven Degree of Freedom Haptic Device for Engineering Design

Seahak Kim, Jeffrey Berkley

MIMIC Technologies Inc., Seattle, WA, USA

Key Words: Force Feedback, Haptics, Virtual Design, CAE

In this paper, the authors intend to demonstrate a new intuitive force-feedback device that is ideally suited for engineering design. Force feedback for the device is tension-based and is characterized by 7 degrees of freedom (3 DOF for translation, 3 DOF for rotation, and 1 DOF for grasp). The SPIDAR-G (**S**pace **I**nterface **D**evice for **A**rtificial **R**eality with **G**rip) allows users to interact with virtual objects naturally by manipulating two hemispherical grips located in the center of a device frame. Force feedback is achieved by controlling tension in strings that are connected between a grip and motors located at the corners of a frame. Methodologies will be discussed for displaying force and calculating translation, orientation and grasp using the length of 8 connecting strings. The SPIDAR-G is characterized by smooth force feedback, minimized inertia, no backlash, scalability and safety. Such features are attributed to strategic string arrangement and control that results in stable haptic rendering. Experimental results validate the feasibility of the proposed device and example applications are described.

1. Introduction

Computer aided design (CAD) software has proliferated due to its potential advantages over physical modeling. Design within software is not susceptible to many of the problems inherent to physical models; “materials” won’t shrink, break or melt and there is no need to wait for paints, glues

and clay to dry. In the computer you have the “undo” option when a mistake is made and repetitive work can be “copied”. Scaling, distortion and automated smoothing are features not available in physical modeling. However, despite the advantages of CAD, many engineers often prefer physical model design. This is because the computer interface does not easily facilitate 3D design. The mouse and computer screen allow only 2D visualization and navigation, which can be cumbersome for creating 3D objects.

Imagine trying to tell Michel Angelo to sculpt *David* within the confines of the computer interface. This would be equivalent to restricting him to the use of only one eye since the monitor only provides 2D images and to the use of only one arm since he works through the mouse. It would be necessary to disengage his nerve endings because the mouse provides no force feedback and his arm must be confined so that it can only move in one plane at a time. Michel might be able to create a computer model of *David*, but it is likely to take him a substantially longer period of time. This is what engineers are faced with today and it is one of the major reasons why physical modeling is still so popular.

Virtual reality (VR) provides a new medium for engineers to create and interact with designs in a manner that is similar to real life. Instead of the 2D computer screen, visualization typically takes place in 3D through shutter glasses or a head mounted display. Rather than using a 2D mouse, VR applications track 3D human motion. Three-dimensional sound is also becoming common. What is lacking from the VR environment is an effective means for simulating the sense of touch, or *haptics*. Like visualization and sound, haptics can enable effective information exchange between man and machine. This can significantly increase an engineer’s efficiency during the design process.

While many haptic devices are beginning to immerse, most are limited in degrees of freedom and/or workspace size. The available devices can be divided into two categories: ground-based and body-based devices. Examples of body-based force-feedback devices are the LRP data glove[1], the

Cybergrasp force feedback glove by Virtual Technologies Inc[2], and the Rutgers Masters (RM-II)[3] developed at Rutgers University. Fundamentally, body-based force feedback devices have the advantage of allowing the user to grasp an object, but also present the disadvantage of not being able to render solid boundaries or represent the weight of an object. Ground-based force-feedback devices can generally be classified as link type, magnetic levitation type, and tension-based type. Examples of ground-based devices include the PHANTOM [4] (serial link type), the Haptic Master [5] (parallel link type), the CyverForce [6] (link type + glove), the Freedom6S [7] (link type + string), and CMU's magnetic force feedback device [8]. The major limitation of the above mentioned devices are that workspace size is limited. Tension-based devices, such as the SPIDAR [9],[10],[11] (string type), are not limited by workspace and are robust in the number of degrees of haptic freedom that can be supported. To date, there is no intuitive force feedback device that displays 7 DOFs of force, which is not limited by workspace size.

The physical act of gripping (or grasping) is fundamental to performing several important functions, including using our hands or tools to hold, squeeze, turn, pry and bend objects. So far, force-feedback devices have presented users with simple ways of representing this grasping function, such as pushing a button. Such simple interaction can be limiting and there is a need for a more intuitive interface. The purpose of this paper is to describe such a tension-based 7 DOF force-feedback device that can allow users to not only to grasp an object, but also to sense the width of an object as in real life object manipulation. The device will be put into context by describing its use with computer aided design software that is currently being developed.

2. Force Display Using Tension

One characteristic of using strings to display forces is that strings only support tension. In other words, the strings can be used to pull, but not push. The number of strings needed for displaying n -

DOF reflective forces can be determined by applying vector closure. When generating an n -dimensional force vector $q \in R^n$ using m -strings, the force vector q can be added to the target object in the format of equation 1.

$$q = [w_1, w_2, \dots, w_m]^T \tau, \quad \text{where } w_i \in R^n \quad (i = 1, \dots, m) \quad \text{and } \tau = (\tau_1, \tau_2, \dots, \tau_m)^T \quad (\text{Eq. 1})$$

w_i represents a force vector when unit tension is added to the i -th string and τ is the tension vector.

Because strings can only support tension, it is necessary to find a solution where all strings are pulling rather than pushing. In order to realize a positive solution for any τ when $A = [w_1, w_2, \dots, w_m]$, the following indispensable conditions must be met:

1. $m > n$
2. $\text{rank}(A) = n$

A proof of these conditions can be found in the literature [12], [13].

Given the above conditions, any w_i ($i = 1, \dots, n + 1$) can be represented as

$$w_i = - \sum_{j=1(j \neq i)}^{n+1} \alpha_j w_j \quad (\alpha_j > 0) \quad (\text{Eq. 2})$$

However, n is the dimension of the work coordinate. Therefore, it can be conclude that for the user to move an object in any direction in 3-dimensional space, $n+1$ strings are needed. In the case of the SPIDAR-G, at least 8 strings are required to display 7 DOF.

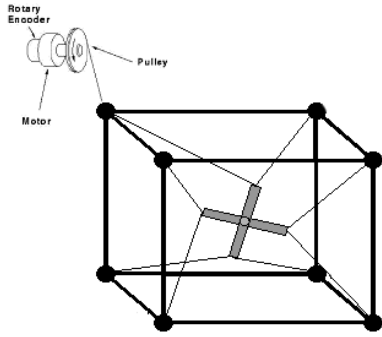


Figure 1. Basic structure of the SPIDAR-G.



Figure 2. State of grip before grasping (left) and after grasping (right)

3. Structure of SPIDAR-G

Although it has been deduced that it was sufficient to use only 8 strings for 7 DOF and that the connection has to comply with conditions of vector closure, it is still necessary to choose the best possible configuration for the connection of strings. The force magnitude, direction and workspace area depend on the way strings are connected between the frame and grip. In general, it can be assumed that the users of the device will work in the central region of the frame. The simplest way to display 7 DOF force in the central area of the frame is by using low torque. In other words, if the position vector of grip was set to $A(\in R^{7 \times 8})$, the larger the result of $\det|A^T A|$, the better it is for our purpose. Using this type of analysis, it is best to connect strings between a vertex of a grip and a corner of a frame, as shown in figure 1. At each corner of the frame, an encoder and a motor are attached to a string. With such an arrangement, the encoders calculate the length of the strings and the motors produce tension by pulling on the strings, enabling 7 DOF force display at the grip.

Human beings are naturally skilled at grasping objects using their thumb and fingers. To display feedback force on the individual fingers, the authors initially tried attaching strings to the tips of each finger. This approach was not very successful as it proved to be difficult to display translation, rotational, and grasping forces using a minimum number of strings.

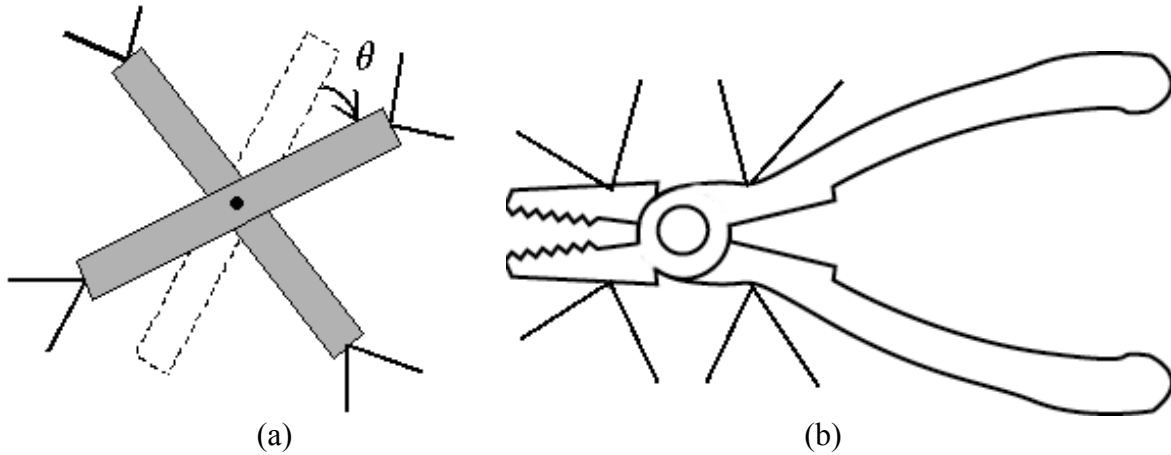


Figure 3. a) Arbitrary grasp manipulator with strings connected to the grip vertices. b) An example of another tool, which incorporates grip.

In this paper the authors suggest a new mechanism for the grip. The grip allows users to manipulate objects over 7 DOFs by grasping a grip between the thumb and other fingers. In order to generalize the “grasping” functionality of the grip to most applications, it is useful to consider a spherical shape. In figure 2, the proposed mechanism is broken into 2 hemispheres that enclose a cross type structure. If the user grasps the grip using thumb and fingers, the 2 poles of the cross rotate depending on the magnitude of the grasp force. Hence, it is possible to control the grasp functionality of the grip. The basic structure of the cross type grip is shown in figure 3a. The grip can also be adapted to various tools as demonstrates in figure 3b. The crossing degree, θ , changes with the magnitude of the grasping force and is used to quantify the action of grasping.

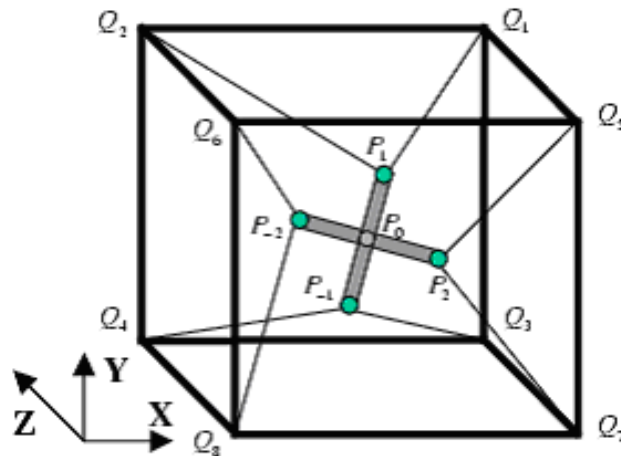


Figure 4. Demonstrates the configuration of the SPIDAR-G with a description of variable names.

4. Calculation of Position

Position (translation, rotation, and grasp) is calculated from the length of 8 strings. The frame has side lengths (along the X, Y and Z axis) represented as $2a, 2b, 2c$. The center of the frame is taken to be at the origin $(0, 0, 0)$. Each position vector Q_i ($\in R^3$) in the i -th extremity of the frame can be represented as follows:

$$Q_1 = (a, b, c), \quad Q_2 = (-a, b, c) \quad (\text{Eq. 3a,b})$$

$$Q_3 = (a, -b, c), \quad Q_4 = (-a, -b, c) \quad (\text{Eq. 3c,d})$$

$$Q_5 = (a, b, -c), \quad Q_6 = (-a, b, -c) \quad (\text{Eq. 3e,f})$$

$$Q_7 = (a, -b, -c), \quad Q_8 = (-a, -b, -c) \quad (\text{Eq. 3g,h})$$

Position vectors of the grip (P_0) and the 4 extremities (P_1, P_{-1}, P_2, P_{-2}), P_i ($\in R^3$) are defined below.

$$P_0 = (x, y, z) \quad (\text{Eq. 4a})$$

$$P_1 = (x + x_1, y + y_1, z + z_1) \quad (\text{Eq. 4b})$$

$$P_{-1} = (x - x_1, y - y_1, z - z_1) \quad (\text{Eq. 4c})$$

$$P_2 = (x + x_2, y + y_2, z + z_2) \quad (\text{Eq. 4d})$$

$$P_{-2} = (x - x_2, y - y_2, z - z_2) \quad (\text{Eq. 4e})$$

If the length of each pole in the cross grip is set to $2d$, then equation 5 can be derived.

$$x_1^2 + y_1^2 + z_1^2 = x_2^2 + y_2^2 + z_2^2 = d^2 \quad (\text{Eq. 5})$$

The grip extremities (P_i) are connected to the i -th frame corners (Q_i). The connectivity is described in figure 4. The length of the i -th string is represented as l_i , as shown in the following equation.

$$l_i = \|Q_i - P_{(i)}\| \quad (i = 1, \dots, 8) \quad (\text{Eq. 6})$$

To calculate translation, rotation, and grasp, (x, y, z) , (x_1, y_1, z_1) , and (x_2, y_2, z_2) must be solved from the length of 8 strings. Equation 6 can be used to obtain equations 7a-g.

$$(x + x_1 - a)^2 + (y + y_1 - b)^2 + (z + z_1 - c)^2 = l_1^2 \quad (\text{Eq. 7a})$$

$$(x + x_1 + a)^2 + (y + y_1 - b)^2 + (z + z_1 - c)^2 = l_2^2 \quad (\text{Eq. 7b})$$

$$(x - x_1 - a)^2 + (y - y_1 + b)^2 + (z - z_1 - c)^2 = l_3^2 \quad (\text{Eq. 7c})$$

$$(x - x_1 + a)^2 + (y - y_1 + b)^2 + (z - z_1 - c)^2 = l_4^2 \quad (\text{Eq. 7d})$$

$$(x + x_2 - a)^2 + (y + y_2 - b)^2 + (z + z_2 + c)^2 = l_5^2 \quad (\text{Eq. 7e})$$

$$(x - x_2 + a)^2 + (y - y_2 - b)^2 + (z - z_2 + c)^2 = l_6^2 \quad (\text{Eq. 7f})$$

$$(x + x_2 - a)^2 + (y + y_2 + b)^2 + (z + z_2 + c)^2 = l_7^2 \quad (\text{Eq. 7g})$$

$$(x - x_2 + a)^2 + (y - y_2 + b)^2 + (z - z_2 + c)^2 = l_8^2 \quad (\text{Eq. 7h})$$

The unknown variables above can be solved using 4 arithmetical operations because of the redundancy of strings. The details of this solution are shown in index 1.

5. Display of Force

In this section, a solution is given for determining the tension of the 8 strings that will result in 7 DOF force display at the “cross-type” grip. The force vector $q (\in R^7)$ can be represented as

$$q = (f_x, f_y, f_z, m_x, m_y, m_z, g)^T \quad (\text{Eq. 8})$$

where f_x, f_y, f_z represent translation forces, m_x, m_y, m_z rotation forces, and g is the grasp force.

The tension of strings $\tau_{(i)}$ ($i = 1, \dots, 8$) can be represented in the tension vector τ , as follows:

$$\tau = (\tau_1, \tau_2, \dots, \tau_8)^T \quad (\in R^8) \quad (\text{Eq. 9})$$

w_i is taken to be the force vector generated at the grip. As tension is added to the i -th string, w_i is

defined as

$$w_i = \begin{bmatrix} c_i \\ r_{(i)} \times c_i \\ \delta_i \cdot n \cdot r_{(i)} \times c_i \end{bmatrix} \quad (\text{Eq. 10})$$

where

$$c_i = \frac{Q_i - P_{(i)}}{\|Q_i - P_{(i)}\|} \quad (i = 1, 2, \dots, 8) \quad (\text{Eq. 11})$$

$$r_{(i)} = P_{(i)} - P_0 \quad (\text{Eq. 12})$$

$$\delta_i : \begin{cases} 1 & i = 1, 2, 3, 4 \\ -1 & i = 5, 6, 7, 8 \end{cases} \quad (\text{Eq. 13})$$

$$n = \frac{r_1 \times r_2}{\|r_1 \times r_2\|} \quad (\text{Eq. 14})$$

If $A \in R^{7 \times 8}$ is set into $A = (w_1, w_2, \dots, w_8)$, then the force vector, q can be represented with equation 15.

$$q = A\tau \quad (\text{Eq. 15})$$

To display the force vector q for a cross type grip, it is necessary to solve the tension vector τ and satisfy equation 15. However, the tension vector must be a positive value vector ($\tau_i \geq 0, i = 1, \dots, 8$).

Solving the quadratic expression in equation 16, the tension vector can be obtained.

$$\|q - A\tau\|^2 \rightarrow \min \quad (\text{where } \tau_{\max} > \tau \geq 0) \quad (\text{Eq. 16})$$

The above equation can be expressed in more detail as shown in equation 17. The target function, J , should be minimized to get the best solution.

$$J = \left\| \sum_i f - c_i \right\|^2 + S_0 \left\| \sum_i f - r_{(i)} \times c_i \right\|^2 + S_1 \left\| \sum_i f - \delta_i \cdot n \cdot r_{(i)} \times c_i \right\|^2 + S_2 \sum_i \tau_i^2 \quad (\text{Eq. 17})$$

The constants S_0 , S_1 , and S_2 are control values for rotation, grasp, and continuity. If S_0 is set larger than any other constant, then the SPIDAR-G system will have the best accuracy when displaying rotational force. If S_1 is largest, grasp force accuracy is emphasized. If S_2 is larger than any other constant, force will be more stable.

Because the SPIDAR-G uses the tension of strings to display force, there are certain locations within the frame where the SPIDAR-G cannot display accurate forces. For example, a user might be able to pull the grip completely out of the frame and still receive forces that pull the grip back toward the center. However, due to the string angles at this position, it will not be possible to push away from the frame. So long as a user keeps the grip near the center of frame, the SPIDAR-G will display 7 DOF force appropriately.

6. Evaluation of the SPIDAR-G Accuracy

One configuration of the SPIDAR-G is shown in figure 5. The length of the frame is 48cm, and the radius of grip is 4cm. The computer, which was used with this SPIDAR-G, is based on a Pentium 400 MHz processor. The encoders are HEDS-5540s made by HP. The DC motors are products of Maxon.[14]

The proposed force feedback device calculates the position of the grip based on the length of the strings. Using encoders that can detect 2000 pulses per 1 rotation and pulleys that each have a radius of 8 mm, the resolution for measuring string length is therefore 0.0251327 mm. A length per pulse multiplied by the counter value is the length of string. Hardware variability can lead to error if string length is calculated using this method. When actual lengths were compared to encoder derived lengths,

an error of $6.24 \pm 1.54\%$ was obtained when testing lengths between 10 and 70 cm. To reduce this error, a least squared criterion was utilized to fit data points to a linear curve. Using a single linear curve calibrated for the SPIDAR-G system shown in figure 5, the error for determining string length was reduced to $0.80 \pm 0.4\%$. This error can be attributed to stretching in the strings and uneven winding of the strings around the pulleys. The total error is minimized when working in the center of the frame. Within a 40 cm cubic volume centered in the middle of the frame (see figure 5), it was determined that the position error never exceeded 4 mm.

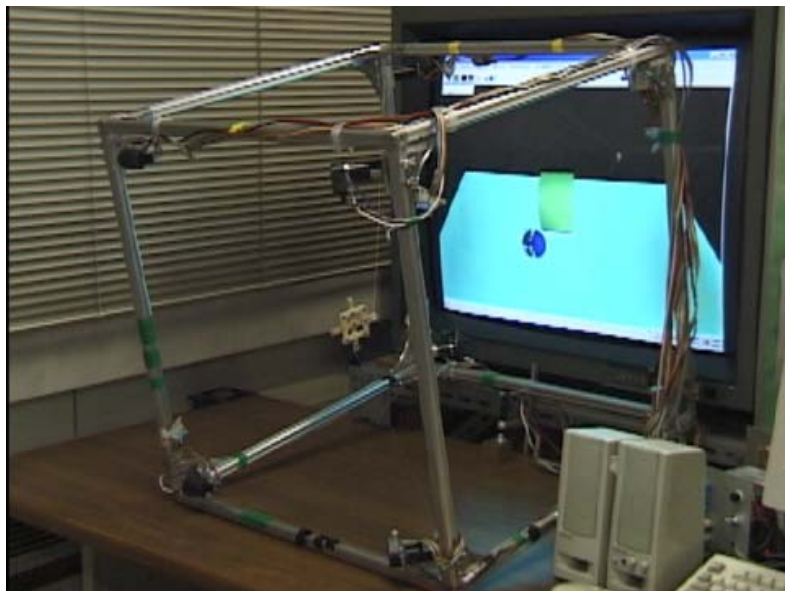


Figure 5. An example of a SPIDAR-G configuration.

The capacity of the SPIDAR-G to deliver a maximum force deteriorates as the user moves the grip away from the center of the workspace. Unfortunately, a simple shaped region cannot describe the workspace of maximum deliverable force due to the way the strings are connected. To give the reader some idea about where forces are at their maximum, forces were tested for each axis in the workspace along vectors of expected force deterioration. For example, when moving the grip along the x-axis in the negative direction (y and z equal 0), it is expected that deliverable force in the negative x direction will diminish the farther left the grip is moved. It was determined that maximum force could be reached along the x and y axis so long as the grip was kept within 10 cm of the origin. Forces went to

zero in the direction of expected deterioration as the grip was moved approximately 23 cm away from the origin. Along the z-axis, maximum force was achieved up to 23 cm away from the origin, but quickly dropped to zero at 25 cm. It was determined that maximum grip force could always be obtained in regions where maximum translation force was possible.

When at the center of the frame, maximum rotational force was achieved up to 45 degrees rotation around any axis. The accuracy for determining orientation was both dependent on magnitude of rotation and distance from the center of the frame. At the center of the frame, rotation measurement error increased to 4.44 % for 45 degrees of rotation. While maintaining a 45 degree rotation, this error increased to 11% as the grip was translated 20 cm from the origin. Rotation accuracy therefore proved to be quite sensitive to the error in predicted string length. Maximum grip force was achieved beyond 45 degrees of rotation so long as the grip was kept within 10 cm of the frame's origin.

7. Applications

Work is underway to integrate the SPIDAR-G design into various “proof of concept” engineering packages. As of now, every applications discussed in this section does not utilize all seven degrees of freedom, but each application shows how force feedback can play an important roll in engineering.

Designing a prototype first begins with creating geometries. Using the mouse cursor to select features, such as points, edges or surfaces, can often be ambiguous since the cursor may lie over several features at one time. For models with complex geometries, selecting the right feature can be very tedious and can reduce design efficiency. With the SPIDAR-G, object selection is as simple as reaching out and touching what the user wants. Force feedback helps a user to stabilize his position of a 3D cursor, which simplifies interaction and makes object manipulation more intuitive. “Snap” helper forces can be used to pull a 3D cursor towards features of interest, which makes it easier to select and

align objects.

Two design packages have been created by the authors to demonstrate the advantages of force-feedback devices like the SPIDAR-G ; a freeform and implicit solid modeler. Figure 6 shows freeform modeling software that allows amorphous shapes to be stretched, twisted and bent into a desired geometry. Because the material properties of the molded material can be adjusted, different stretching and bending parameters can allow for variability not achievable through a physical medium. Computer design is also not limited by continuum mechanics in that the user can choose whether or not to ignore limitations such as conservation of volume.

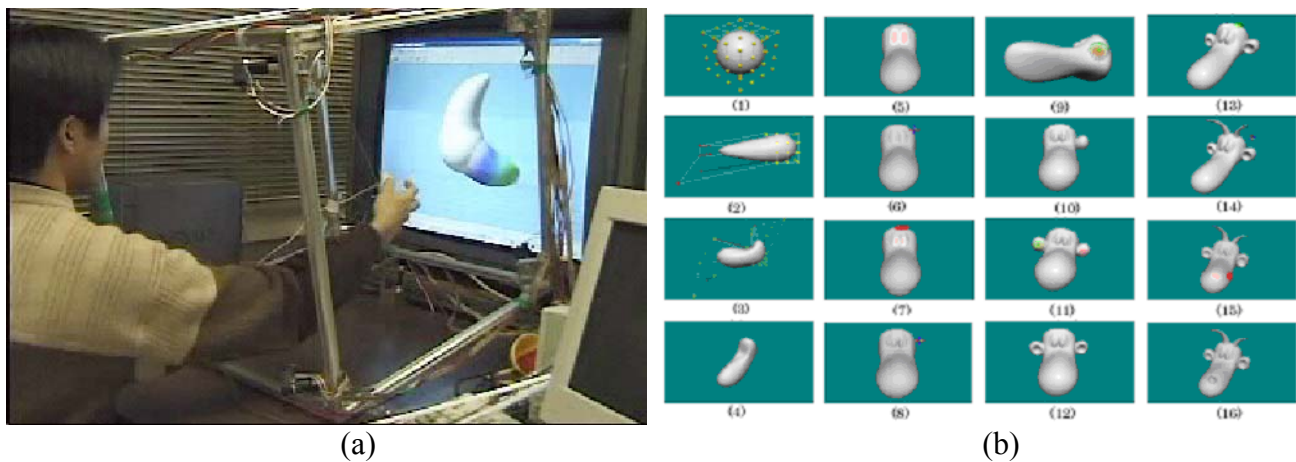


Figure 6. Freeform modeling software can be used with the SPIDAR-G to construct a variety of geometries.

Another popular design methodology involves using primitive shapes defined by mathematical equations to build prototypes. Given 3D coordinates in space, *implicit solid* equations result in a positive value when outside the volume of an object, a negative value when inside, and a zero value when on the surface. This type of representation has many advantages; including efficient collision detection and simplified mesh generation for the analysis phase. Figure 7 shows a wall-mounted platform that was created using solid modeling software that takes advantage of haptics. The application is ideal for visualizing and interacting with design ideas and also for creating finite element meshes.

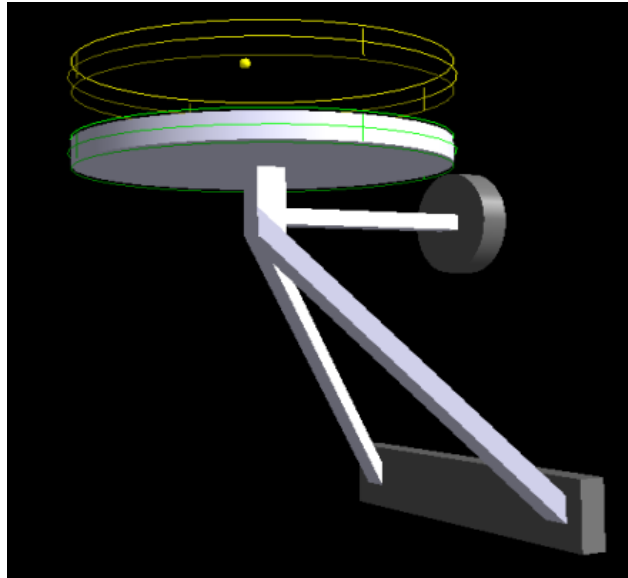


Figure 7. Haptics and 3D navigation can simply design. The above image represents a wall-mounted platform created with haptic enable software developed by the authors.

After creating a design, it is often necessary to perform a thorough analysis to assure that a product will withstand expected wear and tear and also comply with safety standards. Finite element (FE) modeling is an accurate continuum mechanics based methodology that has served as an industry standard for prototype testing and design. Bridges, cars, ships, airplanes, prosthetic devices and mechanical parts represent only a small sample of products that have depended on the accuracy of FE modeling for effective design. While conventional FE modeling is not applicable to real-time rendering for graphics or haptics, FE modeling methodologies that utilize novel preprocessing techniques and alternative real-time solving methodologies are starting to immerge [19-23]. Most of the advances in real-time FE modeling have occurred as a result of the demand for realistic surgery simulation.

The FE method is computationally intensive and requires a substantial amount of time for determining a model's reaction to a set of loading and boundary conditions. Because of computation delay, analysis typically must proceed in a serial manner. For example, when testing a model to find design flaws, an engineer might apply a set of loading conditions, wait for computation to complete, observe the results, and then refine and apply a new set of loading conditions based on previous results.

This procedure might be repeated until the engineer can zero in on problem areas of the design. The process is by no means “interactive”. As time passes, it becomes difficult for the engineer to recall and conceptualize the overall effect of previously applied loading conditions. This deteriorates the engineer’s ability to efficiently conduct a thorough analysis. Real-time FE modeling with haptic support can significantly improve efficiency and help optimize the design process.

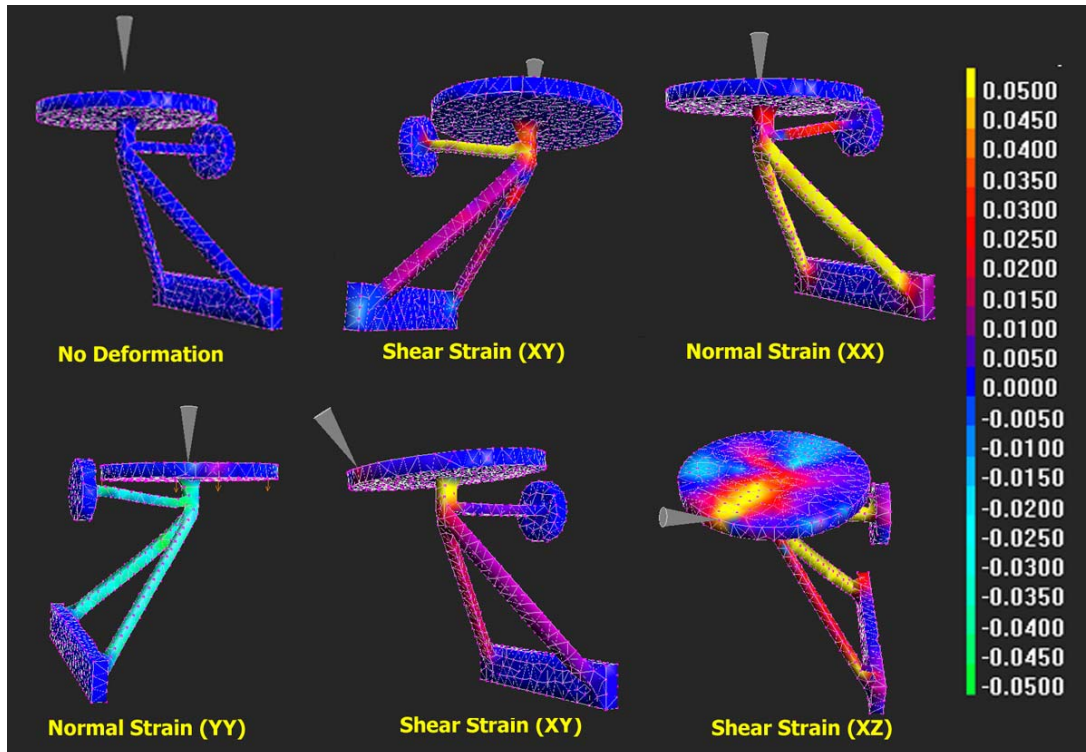


Figure 8. Image captures from a real-time FE analysis package created by the authors. Haptic feedback provides intuitive analysis that is not available in typical software applications.

Figure 8 shows image captures of real-time FE analysis results of a wall-mounted platform. This FE mesh was created using the implicit modeling software discussed earlier. Real-time analysis is based on novel methodologies that allow high-resolution models to be analyzed in a real-time VR environment [20]. Not only does this application allow an engineer to apply a wide range of loading conditions in a minimal amount of time, the user also receives haptic feedback that can convey more information than is available through typical applications. The feel of an object compressing, stretching, bending and twisting can often convey more information about a design than single frame plots or

movies of deformation, stress and/or strain.

Another application that takes advantage of the force feedback capabilities of the SPIDAR-G is shown in figure 9. This application simulates the assembly of a robot toy in a virtual environment. Product mock-up is one of the most common uses of virtual reality in engineering. This application shows that you don't have to stop at visualization, but can also interact with designs before creating a physical prototype. Simulating assembly, disassembly and packaging in VR with haptics can be very valuable and can help prevent costly mistakes before moving to the manufacturing stage.

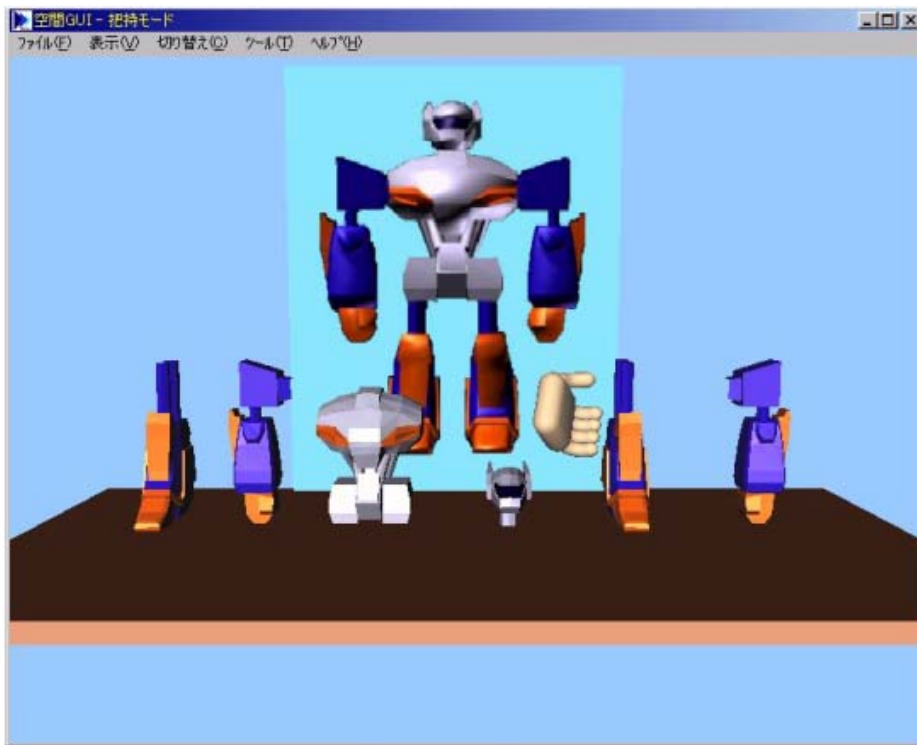


Figure 9. Force feedback can enable assembly simulation in virtual environments. In the image above, the SPIDAR-G is used to assemble a toy robot.

8. Conclusions

A novel 7 DOF haptic device has been proposed that accurately renders force using tension in strings rather than torque through links. Algorithms were presented for determining position based on string length and for displaying force through string tension. The accuracy of the SPIDAR-G was also assessed through simple validation studies. The application of the SPIDAR-G to engineering was

demonstrated through software applications created by the authors. These applications show that force feedback can enhance and optimize many phases of the design process.

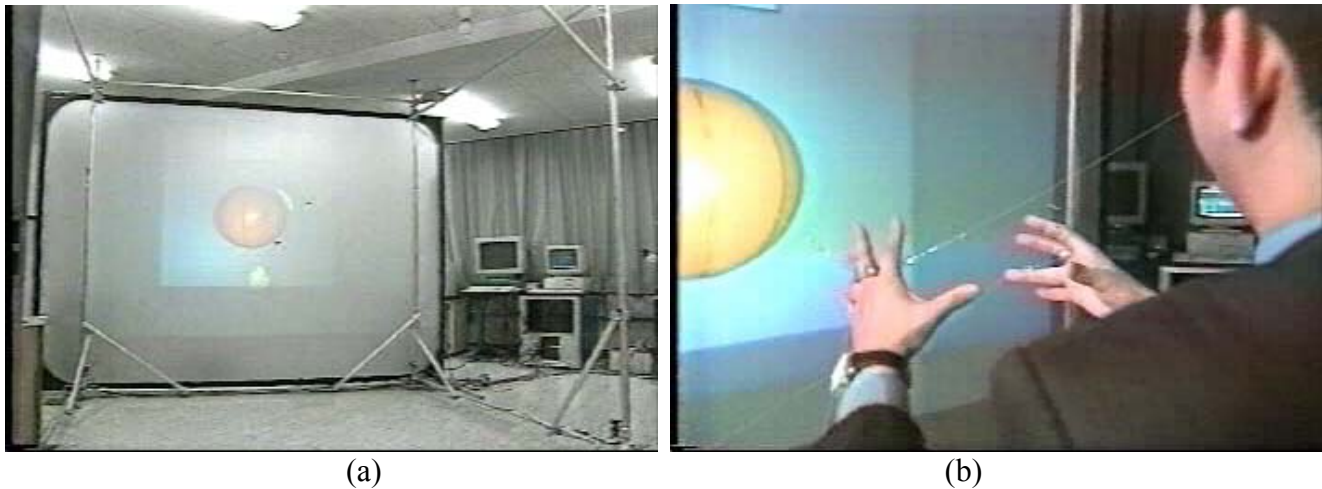


Figure 10. Tension based force feedback devices are scalable, which allows for larger workspaces than linkage-based devices. At the Precision and Intelligence Laboratory at the Tokyo Institute of Technology, various SPIDAR configurations have been constructed that demonstrate the many applications of tension-based force-feedback.

One of the greatest advantages of rendering force through tension is that the haptic workspace is scalable. Linkage-based haptic devices are not suitable for large workspaces. As linkage arms get longer, motors must become stronger to compensate for the increased moments that result from longer lever arms. Tension-based force feedback devices are not susceptible to this problem since forces are applied through linear vectors via strings. A haptic device that uses tension could be the size of a mouse pad or fill an entire room using the same size motors. Strings are also less obtrusive to vision, making haptic devices like the SPIDAR-G ideal for VR environments where virtual objects are collocated with the user's hands through stereoscopic projection. Systems such as the CAVE environment could easily be coupled with tension-based force feedback.

Work is currently underway to expand the capabilities of the software applications described in this paper. With 7 DOF, haptic software functionality can be significantly expanded. Not only have the authors applied the SPIDAR-G and other SPIDAR configurations to engineering applications, they have also begun applying SPIDAR technology to surgery simulation. With up to 7 DOF per tool, there

are now many more surgical procedures that could be simulated with haptics. Entertainment is also a natural application of SPIDAR technology and will receive significant attention in the near future.

References

- [1] Bouzit, M., Coiffet, P. and Burdea, G., The LRP Dextrous Hand Master, Proceedings of VR System'93 Conference, October 1993, New York City.
- [2] <http://www.virtex.com> , (<http://www.immersion.com>)
- [3] Gomez, D., Burdea, G., and Langrana, N., The Second Generation Rutgers Master – RM II, Proceedings of Automation'94 Conference, July 1994, Taipei, Taiwan, Vol. 5, pp.7-10.
- [4] Massie, T., Design of a Three Degree of Freedom Force-Reflecting Haptic Interface. Bachelor of Science thesis, May 1993, Massachusetts Institute of Technology.
- [5] Iwata, H., Artificial Reality with Force-Feedback: Development of Desktop Virtual Space with Compact Master Manipulator. Computer Graphics (SIGGRAPH' 90 Proceeding), 1990, pp.165-170.
- [6] <http://www.immersion.com>
- [7] <http://www.mpb-technologies.ca>
- [8] Berkelman, P., Butler, Z., and Hollis, R., Design of a Hemispherical Magnetic levitation Haptic Interface. DSC-Vol. 58, Proceedings of the ASME Dynamics Systems and Control Division, 1996, pp.483-488.
- [9] Sato, M., Hirata, Y., and Kawarada, H., SPace Interface Device for Artificial Reality-SPIDAR. The Transactions of the Institute of Electronics, Information and Communication Engineers (D-II), July, 1991, J74-D-II, 7, pp.887-894.
- [10] Ishii, M., Nakata, M., and Sato, M., Networked SPIDAR: A Networked Virtual Environment with Visual, Auditory, and Haptic Interaction, PRESENCE (MIT Press Journal), 1994, Vol.3, No.4, pp351-359.
- [11] Bouguila, L., Cai, Y., and Sato, M., New Interface Device For Human-Scale Virtual Environment: Scaleable-SPIDAR. International Conference on Artificial reality and Tele-existence (ICAT97), 1997, pp.93-98, Tokyo.
- [12] Kawamura, S., and Ito, K., A New Type of Master Robot for Teleoperation Using A Radial Wire Drive System. Proceedings of the 1993 IEEE/RSJ International Conference on Intelligent Robots and System, 1993, pp.55-60.
- [13] A.J.Goldman and A.W. Tucker. Polyhedral Convex Cones in Linear Inequalities and Related System. H.W.Kuhn and A.W.Tucker editors, Princeton Univ. Press, 1956.
- [14] Maxon motor catalog, (www.maxonmotor.com)
- [15] Ishii, M., and Sato, M., Force Sensations in Pick-and-Place Tasks. International Conference of American Society of Mechanical Engineering 1994, Chicago, USA, DSC-Vol.55-1, pp.339-344.
- [16] Kim, S., Somsak, W., Ishii, M., Koike, Y., and Sato, M., Personal VR system for rehabilitation to hand movement. International Conference on Artificial reality and Tele-existence (ICAT98), 1998, pp102-108 ,Tokyo.
- [17] Ishii, M., and Sato, M., A 3D spatial Interface device using tensed strings. Presence, 1994, 3(1), pp.81-86.
- [18] Seahak Kim, S. Hasegawa, Y Koike and M. Sato. Tension-based 7 DOFs force feedback device : SPIDAR-G, IEEE VR2002, March, 2002, USA.

- [19] Berkley, J., Ganter, M., Weghorst, S., Gladstone, H., Raugi, G., Berg, D., Real-Time Finite Element Modeling with Haptic Support. in 1999 ASME Design Engineering Technical Conferences. Las Vegas, Nevada.
- [20] Berkley, J., Turkiyyah, G., Berg, D., Ganter, M., Weghorst, S., Real-Time Finite Element Modeling for Graphical and Haptic Rendering: An Application to Surgical Simulation, IEEE Trans. in Visualization and Computer Graphics, 2002, *In Submission*
- [21] Bro-Nielsen, M., Fast finite elements for surgery simulation. Stud Health Technol Inform, 1997, 39: p. 395-400.
- [22] Cotin, S., Delingette, H., and Ayache, N., Efficient linear elastic models of soft tissue for real-time surgery simulation, INRIA, Institute national de Recherche en Informatique et en Automatique, 1998.
- [23] Basdogan, C., Real-Time Simulation of Dynamically Deformable Finite Element Models Using Modal Analysis and Spectral Lanczos Decomposition Methods, in Medicine Meets Virtual Reality. 2001. Newport Beach, CA.

Index 1

The variables x, y, x_1 and y_2 can be obtained by adding equations 7a-h together to cancel terms.

$$x = \text{eq}(7a) + \text{eq}(7b) + \text{eq}(7c) + \text{eq}(7d) \quad (\text{Eq. 18a})$$

$$y = \text{eq}(7a) + \text{eq}(7b) - \text{eq}(7c) - \text{eq}(7d) \quad (\text{Eq. 18b})$$

$$x_1 = \text{eq}(7e) + \text{eq}(7f) + \text{eq}(7g) + \text{eq}(7h) \quad (\text{Eq. 18c})$$

$$y_2 = \text{eq}(7e) - \text{eq}(7f) + \text{eq}(7g) - \text{eq}(7h) \quad (\text{Eq. 18d})$$

Therefore,

$$x = \frac{1}{8a} (-l_1^2 + l_2^2 - l_3^2 + l_4^2) \quad (\text{Eq. 19a})$$

$$y = \frac{1}{8a} (-l_5^2 - l_6^2 + l_7^2 + l_8^2) \quad (\text{Eq. 19b})$$

$$x_1 = \frac{1}{8a} (-l_1^2 + l_2^2 + l_3^2 - l_4^2) \quad (\text{Eq. 19c})$$

$$y_2 = \frac{1}{8a} (-l_5^2 + l_6^2 + l_7^2 - l_8^2) \quad (\text{Eq. 19d})$$

Four equations can be obtained for z . These 4 equations can be changed into 2 six-variable equations. In general, an iterative solution can be used to solve six-variable equations. However, this method requires suitable conditions, substantial time due to the iterative nature of the technique, and the results are only approximations. It is necessary to reduce the amount of calculations to maintain the haptic servo loop and precise results are needed rather than approximations in order to earn high resolution. Iterative numerical methodologies are therefore unsuitable. Fortunately, in the case of using strings, the above 2 six-variable equations contain the same result about z due to the redundancy of the strings. By either adding or subtracting 2 equations, it is possible to obtain a six-variable equation and a five variable equation, which have a common solution about z . By dividing the high variable equation

by the low variable equation, we get the result of z . Using this, the other variables (y_1, z_1, x_2, y_2, z_2) can be solved.

$$y_1 = \frac{1}{2b} \{k_1 + (z - c)^2\} \quad (\text{Eq. 20a})$$

$$x_2 = \frac{1}{2a} \{k_2 + (z + c)^2\} \quad (\text{Eq. 20b})$$

$$y_2 = \frac{1}{8b} (-l_5^2 + l_6^2 + l_7^2 - l_8^2) \quad (\text{Eq. 20c})$$

$$z_2 = \left\{ \frac{1}{8} (l_5^2 - l_6^2 + l_7^2 - l_8^2) - yy_2 - ax - xx_2 \right\} / (z + c) \quad (\text{Eq. 20d})$$

where

$$k_1 = x^2 + y^2 + d^2 + a^2 + b^2 - \frac{1}{4} \sum_{i=1}^4 l_i^2 \quad (\text{Eq. 21a})$$

$$k_2 = x^2 + y^2 + d^2 + a^2 + b^2 - \frac{1}{4} \sum_{i=5}^8 l_i^2 \quad (\text{Eq. 21b})$$